J|A|C|S
ARTICLES
Published on Web 09/26/2006

Kinetics and Mechanism of Ketone Enolization Mediated by Magnesium Bis(hexamethyldisilazide)

Xuyang He, J. Jacob Morris, Bruce C. Noll, Seth N. Brown,* and Kenneth W. Henderson*

Contribution from the Department of Chemistry and Biochemistry, University of Notre Dame, Notre Dame, Indiana 46556-5670

Received July 18, 2006; E-mail: khenders@nd.edu

Abstract: Magnesium bis(hexamethyldisilazide), $Mg(HMDS)_2$, reacts with substoichiometric amounts of propiophenone in toluene solution at ambient temperature to form a 74:26 mixture of the enolates (*E*)- and (*Z*)-[$(HMDS)_2Mg_2(\mu$-HMDS)$\{\mu$-OC(Ph)=$CHCH_3\}$], (*E*)-**1** and (*Z*)-**1**, which contain a pair of three-coordinate metal centers bridged by an amide and an enolate group. The compositions of (*E*)-**1** and (*Z*)-**1** were confirmed by solution NMR studies and also by crystallographic characterization in the solid state. Rate studies using UV−vis spectroscopy reveal the rapid and complete formation of a reaction intermediate, **2**, between the ketone and magnesium, which undergoes first-order decay with rate constants independent of the concentration of excess $Mg(HMDS)_2$ ($\Delta H^{\ddagger} = 17.2 \pm 0.8$ kcal/mol, $\Delta S^{\ddagger} = -11 \pm 3$ cal/mol·K). The intermediate **2** has been characterized by low-temperature ^{1}H NMR, diffusion-ordered NMR, and IR spectroscopy and investigated by computational studies, all of which are consistent with the formulation of **2** as a three-coordinate monomer, $(HMDS)_2Mg\{\eta^1$-O=C(Ph)$CH_2CH_3\}$. Further support for this structure is provided by the synthesis and structural characterization of two model ketone complexes, $(HMDS)_2Mg(\eta^1$-O=C^{t}Bu$_2$) (**3**) and $(HMDS)_2Mg\{\eta^1$-O=C(^{t}Bu)Ph$\}$ (**4**). A large primary deuterium isotope effect ($k_H/k_D =$ 18.9 at 295 K) indicates that proton transfer is the rate-limiting step of the reaction. The isotope effect displays a strong temperature dependence, indicative of tunneling. In combination, these data support the mechanism of enolization proceeding through the single intermediate **2** via intramolecular proton transfer from the α carbon of the bound ketone to the nitrogen of a bound hexamethyldisilazide.

Introduction

The development of synthetic methods for the selective generation of enolate anions is an area of active interest due to the great utility of these synthons in carbon−carbon bond forming reactions.[1] Lithium amides, such as lithium diisopropylamide (LDA), lithium 2,2,6,6-tetramethylpiperidide (LTMP), and lithium hexamethyldisilazide (LiHMDS), have evolved to become the dominant bases of choice to mediate kinetic enolization reactions.[2,3] These reagents are highly selective in the deprotonation of ketonic substrates as they combine the properties of relatively large steric encumbrance,[4] strong Brønsted basicity,[5] and low nucleophilicity. Numerous theoretical,[6] solid-state,[7,8] solution,[9] and kinetic investigations[10] of lithium-mediated enolizations have revealed an astonishing degree of complexity underlying these seemingly simple transformations. In this regard, the systematic spectroscopic and mechanistic studies of lithium amide-mediated enolization reactions by Collum are particularly revealing.[11−13] The picture that has emerged from this work is that no single mechanism is adequate

(1) (a) Heathcock, C. H. In *Comprehensive Organic Synthesis*; Trost, B. M., Fleming, I., Eds.; Pergamon: Oxford, 1991; Vol. 2, p 181. (b) Caine, D. In *Comprehensive Organic Synthesis*; Trost, B. M., Fleming, I., Eds.; Pergamon: Oxford, 1991; Vol. 3, p 1. (c) d'Angelo, J. *Tetrahedron* **1976**, *32*, 2979. (d) Morrison, J. D., Ed. *Asymmetric Synthesis*; Academic: New York, 1983; Vols. 2 and 3. (e) Snieckus, V. *Chem. Rev.* **1990**, *90*, 879.

(2) (a) Berrisford, D. J. *Angew. Chem., Int. Ed. Engl.* **1995**, *34*, 178. (b) Clayden, J. *Organolithiums: Selectivity for Synthesis*; Pergamon: Oxford, 2002. (c) Schlosser, M., Ed. *Organometallics in Synthesis*; Wiley: New York, 2002; Chapter 1. (d) Wakefield, B. J. *Organolithium Methods;* Academic: London, 1988.

(3) For reviews on enantioselective deprotonations mediated by chiral lithium amide bases, see: (a) O'Brien, P. *J. Chem. Soc., Perkin Trans. 1* **1998**, 1439. (b) O'Brien, P. *J. Chem. Soc., Perkin Trans. 1* **2001**, 95. (c) Cox, P. J.; Simpkins, N. S. *Tetrahedron: Asymmetry* **1991**, *2*, 1.

(4) For solution aggregation studies of lithium amides, see: (a) Collum, D. B. *Acc. Chem. Res.* **1993**, *26*, 227. (b) Collum, D. B. *Acc. Chem. Res.* **1992**, *25*, 448. (c) Lucht, B. L.; Collum, D. B. *Acc. Chem. Res.* **1999**, *32*, 1035. (d) Hilmersson, G. *Chem.—Eur. J.* **2000**, *6*, 3069. (e) Zune, C.; Dubois, P.; Grandjean, J.; Kriz, J.; Dybal, J.; Lochmann, L.; Janata, M.; Vlcek, P.; Jerome, R. *Macromolecules* **1999**, *32*, 5477.

(5) For data related to quantitative ion-pair acidity measurements using lithium amides, see: (a) Furlong, J. J. P.; Lewkowicz, E. S.; Nudelman, N. S. *J. Chem. Soc., Perkin Trans. 2* **1990**, 1461. (b) Streitwieser, A.; Juaristi, E.; Nebenzahl, L. In *Comprehensive Carbanion Chemistry*; Buncel, E., Durst, T., Eds.; Elsevier: New York, 1980; Chapter 7. (c) Fraser, R. R.; Baignee, A.; Bresse, M.; Hata, K. *Tetrahedron Lett.* **1982**, *23*, 4195. (d) Fraser, R. R.; Bresse, M.; Mansour, T. S. *J. Chem. Soc., Chem. Commun.* **1983**, 620. (e) Fraser, R. R.; Bresse, M.; Mansour, T. S. *J. Am. Chem. Soc.* **1983**, *105*, 7790. (f) Fraser, R. R.; Mansour, T. S. *J. Org. Chem.* **1984**, *49*, 3442. (g) Fraser, R. R.; Mansour, T. S.; Savard, S. *J. Org. Chem.* **1985**, *50*, 3232. (h) Fraser, R. R.; Mansour, T. S. *Tetrahedron Lett.* **1986**, *27*, 331.

(6) (a) Jemmis, E. D.; Gopakumar, G. In *The Chemistry of Organolithium Compounds*; Rappoport, Z., Patai, S., Eds; Wiley: New York, 2004; Chapter 1. (b) Moreland, D. W.; Dauben, W. G. *J. Am. Chem. Soc.* **1985**, *107*, 2264. (c) Pratt, L. M.; et al. *J. Org. Chem.* **2003**, *68*, 6387. (d) Yakimansky, A. V.; Muller, A. H. E. *J. Am. Chem. Soc.* **2001**, *123*, 4932. (e) Weiss, H.; Yakimansky, A. V.; Muller, A. H. E. *J. Am. Chem. Soc.* **1996**, *118*, 8897. (f) McKee, M. L. *J. Am. Chem. Soc.* **1987**, *109*, 559.

(7) For reviews on lithium enolate structural chemistry, see: (a) Seebach, D. *Angew. Chem., Int. Ed. Engl.* **1988**, *27*, 1624. (b) Williard, P. G. In *Comprehensive Organic Synthesis*; Trost, B. M., Fleming, I., Eds.; Pergamon: Oxford, 1991; Vol. 1, p 1. (c) Fromm, K. M.; Gueneau, A. D. *Polyhedron* **2002**, *23*, 1479.

to describe these proton transfer processes. Almost every aspect of an enolization may affect its mechanism, including the steric and electronic nature of the base and the substrate,[14] the aggregation state of the metal amide, the temperature, the solvent, and the presence of additives, such as salts or cosolvents.[15,16] Another complication is that the mechanism may change as the reaction progresses since the composition of the species present in solution can vary with the extent of reaction.[11g] These complexities are characteristic of organolithium chemistry, where the relatively ionic bonding, combined with the metal's monovalency, leads to intra- and intermolecular fluxionality.[17,18]

Our group has had a longstanding interest in the use of magnesium bis(amides), $Mg(NR_2)_2$, as alternatives to lithium amides in enolization reactions.[19,20] Using a divalent metal reagent allows one greater latitude in tuning the ancillary ligands. Judicious choice of ancillary ligands, coupled with the greater covalency of bonds to magnesium compared to lithium,[21] allows access to systems with simpler solution aggregation behavior and higher thermal stability.[22] We and others have demonstrated the utility of magnesium bis(amide) bases in the regio- and stereoselective deprotonation of ketones,[23,24] as well as with other substrates, including substituted aromatics,[25] cubanes[25a,26] and indoles.[27] Eaton has shown that alkylmagnesium amides are useful in the regioselective deprotonation of weakly acidic substrates, such as cyclopropane and cyclobutane carboxamides.[28] We have also developed a series of homochiral magnesium bis(amide) reagents that have proven to be highly selective in the enantioselective deprotonation of conformationally locked ketones.[29] Other emerging applications of homochiral magnesium amide reagents in asymmetric synthesis include aminations,[30] conjugate additions,[31] alkylations,[32] and reductions.[33] Mixed alkali/alkaline earth metal amide complexes[34] have also very recently been highlighted as regioselective bases in the deprotonation of ketones,[35] arenes,[36] and metallocenes.[37] In addition, magnesium amides have been employed with some success as catalysts in anionic[38] and ring-opening polymerization reactions.[39]

(8) (a) Williard, P. G.; Carpenter, G. B. *J. Am. Chem. Soc.* **1985**, *107*, 3345. (b) Seebach, D.; Amstutz, R.; Laube, T.; Schweizer, W. B.; Dunitz, J. D. *J. Am. Chem. Soc.* **1985**, *107*, 5403. (c) Laube, T.; Dunitz, J. D.; Seebach, D. *Helv. Chim. Acta* **1985**, *68*, 1373. (d) Jastrzebski, J. T. B. H.; Van Koten, G.; Christophersen, M. J. N.; Stam, C. H. *J. Organomet. Chem.* **1985**, *292*, 319. (e) Amstutz, R.; Dunitz, J. D.; Laube, T.; Schweizer, W. B.; Seebach, D. *Chem. Ber.* **1986**, *119*, 434. (f) Williard, P. G.; Hintze, M. J. *J. Am. Chem. Soc.* **1987**, *109*, 5539.

(9) For solution studies of lithium enolates, see: (a) Sato, D.; Kawasaki, H.; Shimada, I.; Arata, Y.; Okamura, K.; Date, T.; Koga, K. *J. Am. Chem. Soc.* **1992**, *114*, 761. (b) Suzuki, M.; Koyama, H.; Noyori, R. *Bull. Chem. Soc. Jpn.* **2004**, *77*, 259. (c) Suzuki, M.; Koyama, H.; Noyori, R. *Tetrahedron* **2004**, *60*, 1571.

(10) (a) Held, G.; Xie, L. *Microchem. J.* **1997**, *55*, 261. (b) Xie, L.; Saunders, W. H., Jr. *J. Am. Chem. Soc.* **1991**, *113*, 3123. (c) Beutelman, H. P.; Xie, L.; Saunders, W. H., Jr. *J. Org. Chem.* **1989**, *54*, 1703. (d) Majewski, M.; Nowak, P. *Tetrahedron Lett.* **1998**, *39*, 1661.

(11) For kinetic studies, see: (a) McNeil, A. J.; Collum, D. B. *J. Am. Chem. Soc.* **2005**, *127*, 5655. (b) Zhao, P. J.; Condo, A.; Keresztes, I.; Collum, D. B. *J. Am. Chem. Soc.* **2004**, *126*, 3113. (c) Zhao, P. J.; Lucht, B. L.; Kenkre, S. L.; Collum, D. B. *J. Org. Chem.* **2004**, *69*, 242. (d) Zhao, P. J.; Collum, D. B. *J. Am. Chem. Soc.* **2003**, *125*, 14411. (e) Zhao, P. J.; Collum, D. B. *J. Am. Chem. Soc.* **2003**, *125*, 4008. (f) Sun, X. F.; Collum, D. B. *J. Am. Chem. Soc.* **2000**, *122*, 2452. (g) Sun, X. F.; Collum, D. B. *J. Am. Chem. Soc.* **2000**, *122*, 2459. (h) Sun, X. F.; Kenkre, S. L.; Remenar, J. F.; Gilchrist, J. H.; Collum, D. B. *J. Am. Chem. Soc.* **1997**, *119*, 4765.

(12) For solution NMR studies, see: (a) Kim, Y. J.; Bernstein, M. P.; Roth, A. S. G.; Romesberg, F. E.; Williard, P. G.; Fuller, D. J.; Harrison, A. T.; Collum, D. B. *J. Org. Chem.* **1991**, *56*, 4435. (b) Galiano-Roth, A. S.; Kim, Y. J.; Gilchrist, J. H.; Harrison, A. T.; Fuller, D. J.; Collum, D. B. *J. Am. Chem. Soc.* **1991**, *113*, 5053. (c) McNeil, A. J.; Toombes, G. E. S.; Chandramouli, S. V.; Vanasse, B. J.; Ayers, T. A.; O'Brien, M. K.; Lobkovsky, E.; Gruner, S. M.; Marohn, J. A.; Collum, D. B. *J. Am. Chem. Soc.* **2004**, *126*, 5938.

(13) For selectivity and theoretical studies, see: (a) Romesberg, F. E.; Collum, D. B. *J. Am. Chem. Soc.* **1995**, *117*, 2166. (b) Hall, P. L.; Gilchrist, J. H.; Collum, D. B. *J. Am. Chem. Soc.* **1991**, *113*, 9571.

(14) (a) Xie, L. F.; Vanlandeghem, K.; Isenberger, K. M.; Bernier, C. *J. Org. Chem.* **2003**, *68*, 641. (b) Xie, L. F.; Isenberger, K. M.; Held, G.; Dahl, L. M. *J. Org. Chem.* **1997**, *62*, 7516.

(15) (a) Seebach, D.; Beck, A. K.; Studer, A. *Mod. Synth. Methods* **1995**, *7*, 1. (b) Loupy, A.; Tchoubar, B. *Salt Effects in Organic and Organometallic Chemistry*; VCH: New York, 1991. (c) Pratt, L. M. *Mini-Reviews in Organic Chemistry* **2004**, *1*, 209.

(16) For studies of mixed anions, see: (a) Romesberg, F. E.; Collum, D. B. *J. Am. Chem. Soc.* **1994**, *116*, 9187. (b) Gilchrist, J. H.; Harrison, A. T.; Fuller, D. J.; Collum, D. B. *Magn. Reson. Chem.* **1992**, *30*, 855. (c) Hall, P. L.; Gilchrist, J. H.; Harrison, A. T.; Fuller, D. J.; Collum, D. B. *J. Am. Chem. Soc.* **1991**, *113*, 9575. (d) Henderson, K. W.; Dorigo, A. E.; Liu, Q. Y.; Williard, P. G.; Schleyer, P. v. R.; Bernstein, P. R. *J. Am. Chem. Soc.* **1996**, *118*, 1339. (e) Sugasawa, K.; Shindo, M.; Noguchi, H.; Koga, K. *Tetrahedron Lett.* **1996**, *37*, 7377. (f) Henderson, K. W.; Walther, D. S.; Williard, P. G. *J. Am. Chem. Soc.* **1995**, *117*, 8680. (g) Henderson, K. W.; Dorigo, A. E.; Liu, Q. Y.; Williard, P. G.; Bernstein, P. R. *Angew. Chem., Int. Ed. Engl.* **1996**, *35*, 1322. (h) Kim, Y. J.; Streitwieser, A. *Org. Lett.* **2002**, *4*, 573.

(17) (a) Stey, T.; Stalke, D. In *The Chemistry of Organolithium Compounds*; Rappoport, Z., Patai, S., Eds.; Wiley: New York, 2004; Chapter 2. (b) Gregory, K.; Schleyer, P. v. R.; Snaith, R. *Adv. Inorg. Chem.* **1991**, *37*, 47. (c) Weiss, E. *Angew Chem., Int. Ed. Engl.* **1993**, *32*, 1501. (d) Beswick, M. A.; Wright, D. S. In *Comprehensive Organometallic Chemistry*; Abel, E. W., Stone, F. G. A., Wilkinson, G., Eds.; Elsevier: Oxford, 1995; Vol. 1, Chapter 1. (e) Boche, G. *Angew. Chem., Int. Ed. Engl.* **1989**, *28*, 277. (f) Mulvey, R. E. *Chem. Soc. Rev.* **1998**, *27*, 339.

(18) Sapse, A. M., Schleyer, P. v. R., Eds. *Lithium Chemistry, A Theoretical and Experimental Overview*; John Wiley & Sons: New York, 1995.

(19) Henderson, K. W.; Kerr, W. J. *Chem. Eur. J.* **2001**, *7*, 3430.

(20) Henderson, K. W.; Allan, J. F.; Kennedy, A. R. *J. Chem. Soc., Chem. Commun.* **1997**, 1149.

(21) Wakefield, B. J. *Organomagnesium Methods in Organic Synthesis*; Academic: London, 1994.

(22) (a) Markies, P. R.; Akkerman, O. S.; Bickelhaupt, F.; Smeets, W. J. J.; Spek, A. L. *Adv. Organomet. Chem.* **1991**, *32*, 147. (b) Westerhausen, M. *Angew. Chem., Int. Ed.* **2001**, *40*, 2975. (c) Lindsell, W. E. In *Comprehensive Organometallic Chemistry*; Wilkinson, G., Stone, F. G. A., Eds.; Pergamon: Oxford, 1982; Vol. 1, Chapter 4.2.

(23) He, X.; Allan, J. F.; Noll, B. C.; Kennedy, A. R.; Henderson, K. W. *J. Am. Chem. Soc.* **2005**, *127*, 6920.

(24) (a) Bonafoux, D.; Bordeau, M.; Biran, C.; Cazeau, P.; Dunogues, J. *J. Org. Chem.* **1996**, *61*, 5532. (b) Lessène, G.; Tripoli, R.; Cazeau, P.; Biran, C.; Bordeau, M. *Tetrahedron Lett.* **1999**, *40*, 4037. (c) Bonafoux, D.; Bordeau, M.; Biran, C.; Dunogues, J. *Synth. Commun.* **1998**, *28*, 93. (d) Bonafoux, D.; Bordeau, M.; Biran, C.; Dunogues, J. *J. Organomet. Chem.* **1995**, *493*, 27.

(25) (a) Eaton, P. E.; Lee, C. H.; Xiong, Y. H. *J. Am. Chem. Soc.* **1989**, *111*, 8016. (b) Kano, T.; Takai, J.; Tokuda, O.; Maruoka, K. *Angew. Chem., Int. Ed.* **2005**, *44*, 3055. (c) Ooi, T.; Uematsu, Y.; Maruoka, K. *J. Org. Chem.* **2003**, *68*, 4576.

(26) Eaton, P. E.; Xiong, Y. H.; Gilardi, R. *J. Am. Chem. Soc.* **1993**, *115*, 10195.

(27) Kondo, Y.; Yoshida, A.; Sakamoto, T. *J. Chem. Soc., Perkin Trans. 1* **1996**, 2331.

(28) (a) Zhang, M. X.; Eaton, P. E. *Angew. Chem., Int. Ed.* **2002**, *114*, 2273. (b) Eaton, P. E.; Zhang, M. X.; Komiya, N.; Yang, C. G.; Steele, I.; Gilardi, R. *Synlett* **2003**, *9*, 1275.

(29) (a) Henderson, K. W.; Kerr, W. J.; Moir, J. H. *Tetrahedron* **2002**, *58*, 4573. (b) Anderson, J. D.; Garcia, P. G.; Hayes, D.; Henderson, K. W.; Kerr, W. J.; Moir, J. H.; Fondekar, K. P. *Tetrahedron Lett.* **2001**, *42*, 7111. (c) Henderson, K. W.; Kerr, W. J.; Moir, J. H. *Synlett* **2001**, 1253. (d) Henderson, K. W.; Kerr, W. J.; Moir, J. H. *Chem. Commun.* **2001**, 1722. (e) Henderson, K. W.; Kerr, W. J.; Moir, J. H. *Chem. Commun.* **2000**, 479. (f) Carswell, E. L.; Hayes, D.; Henderson, K. W.; Kerr, W. J.; Russell, C. J. *SynLett* **2003**, 1017. (g) Bassindale, M. J.; Crawford, J. J.; Henderson, K. W.; Kerr, W. J. *Tetrahedron Lett.* **2004**, *45*, 4175.

(30) Evans, D. A.; Nelson, S. G. *J. Am. Chem. Soc.* **1997**, *119*, 6452.

(31) (a) Sibi, M. P.; Asano, Y. *J. Am. Chem. Soc.* **2001**, *123*, 9708. (b) Bunnage, M. E.; Davies, S. G.; Goodwin, C. J.; Walters, J. A. S. *Tetrahedron: Asymmetry* **1994**, *5*, 35.

(32) Yong, K. H.; Taylor, N. J.; Chong, J. M. *Org. Lett.* **2002**, *4*, 3553.

(33) Yong, K. H.; Chong, J. M. *Org. Lett.* **2002**, *4*, 4139.

(34) (a) Mulvey, R. E. *Chem. Commun.* **2001**, 1049. (b) Mulvey, R. E. *Organometallics* **2006**, *25*, 1060. (c) Clegg, W.; Henderson, K. W.; Mulvey, R. E.; O'Neil, P. A. *J. Chem. Soc., Chem. Commun.* **1993**, 969.

(35) (a) He, X.; Noll, B. C.; Beatty, A.; Mulvey, R. E.; Henderson, K. W. *J. Am. Chem. Soc.* **2004**, *126*, 7444. (b) Hevia, E.; Henderson, K. W.; Kennedy, A. R.; Mulvey, R. E. *Organometallics* **2006**, *25*, 1778.

(36) (a) Krasovskiy, A.; Krasovskaya, V.; Knochel, P. *Angew. Chem., Int. Ed.* **2006**, *45*, 2958. (b) Armstrong, D. R.; Kennedy, A. R.; Mulvey, R. E.; Rowlings, R. B. *Angew. Chem., Int. Ed.* **1999**, *38*, 131. (c) Andrews, P. C.; Kennedy, A. R.; Mulvey, R. E.; Raston, C. L.; Roberts, B. A.; Rowlings, R. B. *Angew. Chem., Int. Ed.* **2000**, *39*, 1960.

(37) (a) Clegg, W.; Henderson, K. W.; Kennedy, A. R.; Mulvey, R. E.; O'Hara, C. T.; Rowlings, R. B.; Tooke, D. M. *Angew. Chem., Int. Ed.* **2001**, *40*, 3902. (b) Hevia, E.; Honeyman, G. W.; Kennedy, A. R.; Mulvey, R. E.; Sherrington, D. C. *Angew. Chem., Int. Ed.* **2005**, *44*, 68. (c) Andrikopoulos, P. C.; Armstrong, D. R.; Clegg, W.; Gilfillan, C. J.; Hevia, E.; Kennedy, A. R.; Mulvey, R. E.; O'Hara, C. T.; Parkinson, J. A.; Tooke, D. M. *J. Am. Chem. Soc.* **2004**, *126*, 11612.

(38) Harder, S.; Feil, F. *Organometallics* **2002**, *21*, 2268.

Despite the increasing interest in these reagents, only very limited mechanistic investigations have appeared,[20,40] and these have mainly focused on the structural characterization of the metal enolate products of the reactions.[23,41] We were therefore interested in conducting a detailed kinetic and mechanistic investigation of magnesium bis(amide)-mediated enolization reactions, using magnesium bis(hexamethyldisilazide), Mg(HMDS)$_2$, as a prototypical magnesium amide.

Mg(HMDS)$_2$ has previously been used as a selective Brønsted base in enolization reactions[23,24a,40,41b] and is readily prepared in a highly pure crystalline form.[42] Westerhausen has established that this compound exists as a mixture of monomers and amide-bridged dimers in arene solutions, with the dimer predominating at ambient temperatures (eq 1).[43] The existence of a well-characterized monomer−dimer equilibrium makes this system particularly amenable to investigating any influence of base aggregation in the deprotonation reaction. Propiophenone was chosen as a representative ketone since it has been used extensively for lithium-mediated methodology development and because stereochemical information may be obtained using this substrate.[14,44] Indeed, we recently reported in a preliminary communication that Mg(HMDS)$_2$ reacts with propiophenone at ambient temperature in toluene solution to give predominantly the (*E*)-enolate (70:30 *E*/*Z*).[23] This is an intriguing result as the corresponding lithium base LiHMDS is known to be highly (*Z*)-selective (2:98 *E*/*Z*).[44a] We also reported that the molecular structure of the amidomagnesium enolate [(HMDS)Mg{μ-OC(Ph)═CHMe}·THF]$_2$ is a centrosymmetric dimer with a central Mg_2O_2 ring.[23]

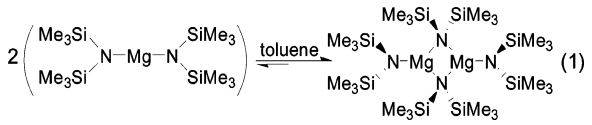

We now report on the mechanistic details of the deprotonation reaction using a combination of spectroscopic, kinetic, computational, and crystallographic methods. These studies provide an unusually coherent and complete description for a metal base-mediated enolization reaction.

Results

Reaction Product Studies. Propiophenone reacts quantitatively with excess Mg(HMDS)$_2$ in toluene solution within 15 min at ambient temperature to form a mixture of two magnesium enolates, (*E*)- and (*Z*)-[(HMDS)$_2$Mg$_2$(μ-HMDS){μ-OC(Ph)═CHCH$_3$}], (*E*)-**1** and (*Z*)-**1** (eq 2 and Figure 1).

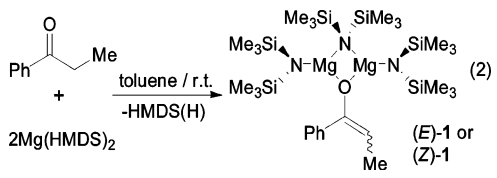

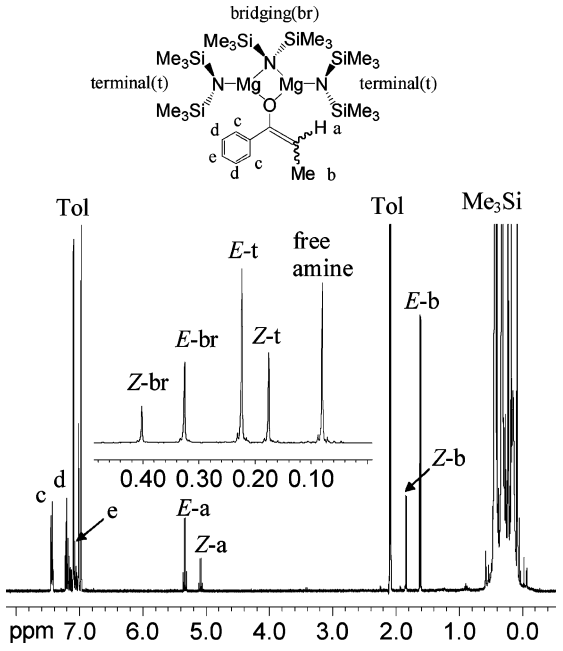

Figure 1. ^{1}H NMR spectra in toluene-d_8 at 298 K of (*E*)-**1** and (*Z*)-**1** prepared in the presence of excess Mg(HMDS)$_2$. The inset shows the trimethylsilyl region from the stoichiometric preparation of (*E*)-**1** and (*Z*)-**1**.

The enolates formed are not the previously characterized bis(enolate)-bridged dimers [(HMDS)Mg{μ-OC(Ph)═CHMe}]$_2$.[23] Instead, the presence of excess Mg(HMDS)$_2$ appears to favor formation of the bimetallics bridged by one enolate and one amide, as judged by the appearance of signals due to terminal and bridging HMDS groups in a 2:1 ratio for each isomer. The presence of two isomers is attributed to (*E*)- and (*Z*)-enolates, in a 74:26 ratio, similar to the ratio of 70:30 measured using 0.75 molar equiv of ketone.[23] The identity of the stereoisomers is assigned by analogy with nOe experiments on other Mg enolates[23] and is confirmed by trapping the enolates as the silyl enol ethers. Direct trapping of the magnesium enolates with Me_3SiCl proved to be very slow in toluene solution. However, transmetalation using BuLi followed by the addition of Me_3SiCl and THF results in quantitative formation of the silyl enol ethers. The stereochemistry of the enolates was confirmed by comparison with authentic samples, and the *E*/*Z* ratio was determined to be 72:28 by GC analyses.[44a]

Reaction of 2 molar equiv of Mg(HMDS)$_2$ with propiophenone in toluene-d_8 was consistent with the formation of (*E*)-**1** and (*Z*)-**1** (inset of Figure 1). Furthermore, this system proved to be amenable to crystallization, and subsequent analysis by X-ray diffraction confirmed their identities in the solid state (Figure 2). The stereoisomers cocrystallize within single crystals giving rise to disorder of the enolate fragment. Similarly, cocrystallization of the (*E*)- and (*Z*)-enolates was found for the bis(enolate)-bridged dimer [(HMDS)Mg{μ-OC(Ph)═CHMe}·THF]$_2$.[23] In the present instance, the best fit

(39) (a) Chisholm, M. H.; Gallucci, J.; Phomphrai, K. *Chem. Commun.* **2003**, 48. (b) Chisholm, M. H.; Gallucci, J. C.; Phomphrai, K. *Inorg. Chem.* **2005**, *44*, 8004. (c) Dove, A. P.; Gibson, V. C.; Marshall, E. L.; White, A. J. P.; Williams, D. J. *Dalton Trans.* **2004**, 570.
(40) Allan, J. F.; Henderson, K. W.; Kennedy, A. R. *Chem. Commun.* **1999**, 1325.
(41) (a) Allan, J. F.; Clegg, W.; Henderson, K. W.; Horsburgh, L.; Kennedy, A. R. *J. Organomet. Chem.* **1998**, *559*, 173. (b) Allan, J. F.; Henderson, K. W.; Kennedy, A. R.; Teat, S. J. *Chem. Commun.* **2000**, 1059.
(42) Nöth, H.; Schlosser, D. *Inorg. Chem.* **1983**, *22*, 2700.
(43) (a) Westerhausen, M. *Coord. Chem. Rev.* **1998**, *176*, 157. (b) Westerhausen, M.; Schwarz, W. *Inorg. Chem.* **1991**, *30*, 96.
(44) (a) Heathcock, C. H.; Buse, C. T.; Kleschick, W. A.; Pirrung, M. C.; Sohn, J. E.; Lampe, J. *J. Org. Chem.* **1980**, *45*, 1066. (b) Brown, H. C.; Dhar, R. J.; Bakshi, R. K.; Pandiarajan, P. K.; Singaram, B. *J. Am. Chem. Soc.* **1989**, *111*, 3441. (c) Fataftah, Z. A.; Kopka, I. E.; Rathke, M. W. *J. Am. Chem. Soc.* **1980**, *102*, 3959. (d) Heathcock, C. H.; Davidsen, S. K.; Hug, K. T.; Flippin, L. A. *J. Org. Chem.* **1986**, *51*, 3027. (e) House, H. O.; Czuba, L. J.; Gall, M.; Lomstead, H. D. *J. Org. Chem.* **1969**, *34*, 2324.

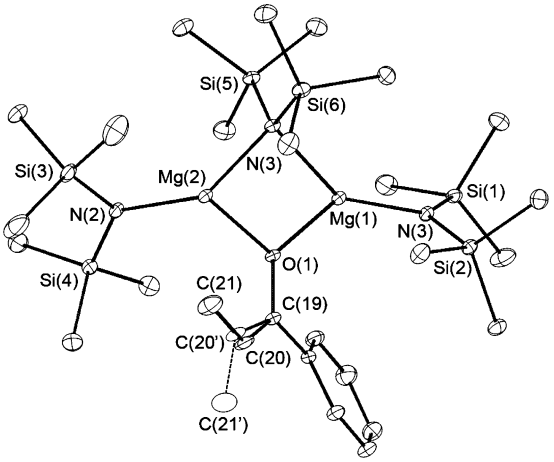

Figure 2. Ellipsoid view (50% probabilities) of **1** with hydrogen atoms omitted for clarity. The methine C(20′) and methyl C(21′) positions for the minor component (*E*)-**1** are shown as hollow ellipsoids.

model for the disorder indicates a 22:78 ratio of the (*E*)- and (*Z*)-isomers within the crystal studied. This ratio differs from that observed from the in situ preparation, suggesting that preferential crystallization is occurring. Indeed, NMR analysis of a representative sample of crystals deposited indicated an approximately 20:80 ratio for the (*E*)- and (*Z*)-enolates. The crystals were isolated in an 11% overall yield, suggesting that the (*E*)-enolate is the more soluble isomer and that it is retained in solution.

The composition of **1** is somewhat unusual, containing two different types of bridging groups between the metals. However, the previously characterized amido(alkoxide) ^{t}BuMg(μ-O^{t}Bu)-(μ-TMP)Mg(TMP) also contains three-coordinate magnesium centers with a central Mg_2ON ring core.[45] The Mg_2ON ring in **1** is slightly puckered, with a Mg(1)−O(1)−Mg(2)−N(3) dihedral angle of 6.8°, and all four ligand groups are tilted out of the mean ring plane. The metrical parameters for **1** are in accord with expectations (Table S1).

Rate Studies. Mixing the colorless reactants, propiophenone and $Mg(HMDS)_2$, in toluene at room temperature immediately produces a bright yellow solution, due to a significant increase in absorbance in the near-UV region. The appearance of color is consistent with the formation of a pre-enolization intermediate, hereafter referred to as **2**, and the color decays over the course of a few minutes, concomitant with formation of the enolate product. The absorbance due to **2** is proportional to the concentration of added propiophenone in the presence of excess $Mg(HMDS)_2$. The absorbance at 330 nm decays exponentially (Figure S1), with a half-life of 139 s ($k_{obs} = (4.99 \pm 0.11) \times 10^{-3}$ s^{-1}) under these conditions (0.048 M $Mg(HMDS)_2$, 4.8×10^{-3} M propiophenone, 21.8 °C).

As expected for a first-order reaction, the observed rate constant is insensitive to the initial concentration of the limiting reagent, propiophenone, in the range 4.87×10^{-4} to 2.92×10^{-3} M. More surprisingly, k_{obs} is also insensitive to the concentration of the excess reagent, $Mg(HMDS)_2$ (Figure 3). These data indicate that **2** decays to enolate in a unimolecular process that is independent of the presence of both monomeric and dimeric forms of $Mg(HMDS)_2$ in the mixture. Solvent

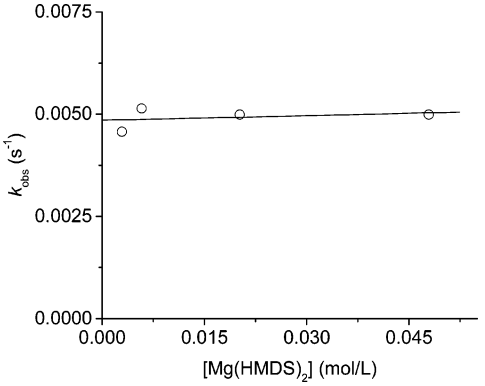

Figure 3. Plot of k_{obs} for the disappearance of **2** versus total concentration of magnesium bis(hexamethyldisilazide) in toluene at 21.8 °C.

polarity has little effect on the rate of decay of **2** with $k_{obs} = (4.93 \pm 0.07) \times 10^{-3}$ s^{-1} at 21.8 °C in CH_2Cl_2 ($\epsilon = 8.9$) identical within experimental error to the value obtained in toluene ($\epsilon = 2.4$).

Deuterium Isotope Effect and Activation Parameters. To measure a kinetic isotope effect on the enolization reaction, α-deuterated propiophenone was prepared by base-catalyzed exchange with CH_3OD.[46] Propiophenone-d_2 reacts much more slowly with $Mg(HMDS)_2$ than the protio compound, with $k_H/k_D = 18.9 \pm 0.6$ at 21.8 °C. This corresponds to a change in half-life from approximately 2.3 to 42 min. (The stereoselectivity of enolization is scarcely affected by deuteration, with $PhCOCD_2CH_3$ reacting to give a 77:23 mixture of (*E*)- and (*Z*)-enolates by NMR.) The primary isotope effect clearly indicates that C−H bond cleavage is involved in the rate-determining step and is large enough to suggest that tunneling is important in this reaction.[47]

Further evidence for tunneling is provided by the temperature dependence of the isotope effect.[48] Experiments were run over the temperature range of 21.8−65.4 °C, and the isotope effect decreases markedly with increasing temperature (for example, to 10.1 at 45.2 °C), as expected for a reaction involving tunneling. Arrhenius plots (Figure 4) give $E_a^D - E_a^H = 2.6 \pm 0.3$ kcal/mol and $A_H/A_D = 0.20 \pm 0.08$. The fact that the $E_a^D - E_a^H$ value significantly exceeds the classical maximum of approximately 1.2 kcal/mol and that the prefactor ratio is significantly smaller than the classical minimum of 0.5[47b] is strong evidence that tunneling is in fact occurring in the proton transfer step.[47,48] Activation parameters for the enolization reaction of the protio compound were derived from an Eyring plot (Figure S2), giving $\Delta H^‡ = 17.2 \pm 0.8$ kcal/mol, $\Delta S^‡ = -11 \pm 3$ cal/mol·K, and $\Delta G^‡$ (295 K) $= 20.4 \pm 1.7$ kcal/mol.

IR and NMR Spectroscopic Characterization of the Enolization Intermediate 2. Addition of propiophenone (α-deuterated to retard enolization) to a toluene solution of $Mg(HMDS)_2$ leads to the appearance of a single IR band in the C═O bond stretching region at 1657 cm^{-1}, which diminishes with time as the enolate is formed. In comparison, the C═O bond stretch in free propiophenone-d_2 appears at 1693 cm^{-1}.

(45) Conway, B.; Hevia, E.; Kennedy, A. R.; Mulvey, R. E.; Weatherstone, S. *Dalton Trans.* **2005**, 1532.

(46) Maestri, A. G. PhD Thesis, University of Notre Dame, 2003, Chapter 4.

(47) (a) Bell, R. P. *The Proton in Chemistry*, 2nd ed.; Cornell University: Ithaca, New York, 1973; Chapter 12. (b) Melander, L.; Saunders, W. H. *Reaction Rates of Isotopic Molecules*; John Wiley & Sons: New York, 1980; Chapter 5.2.

(48) (a) Kaldor, S. B.; Saunders, W. H. *J. Am. Chem. Soc.* **1979**, *101*, 7594. (b) Garcia-Garibay, M. A.; Gamarnik, A.; Bise, R.; Pang, L.; Jenks, W. S. *J. Am. Chem. Soc.* **1995**, *117*, 10264.

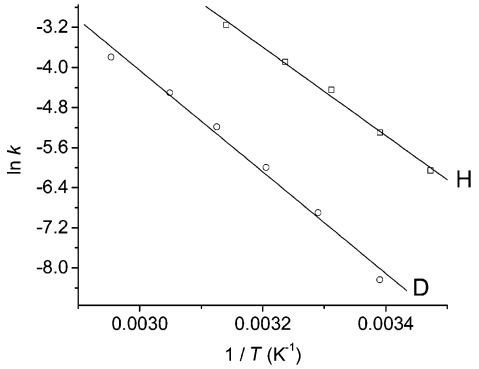

Figure 4. Arrhenius plots of the decay of intermediate **2** formed from the reaction of Mg(HMDS)$_2$ with O═C(Ph)CH$_2$CH$_3$ (squares) and O═C(Ph)CD$_2$-CH$_3$ (circles) in toluene.

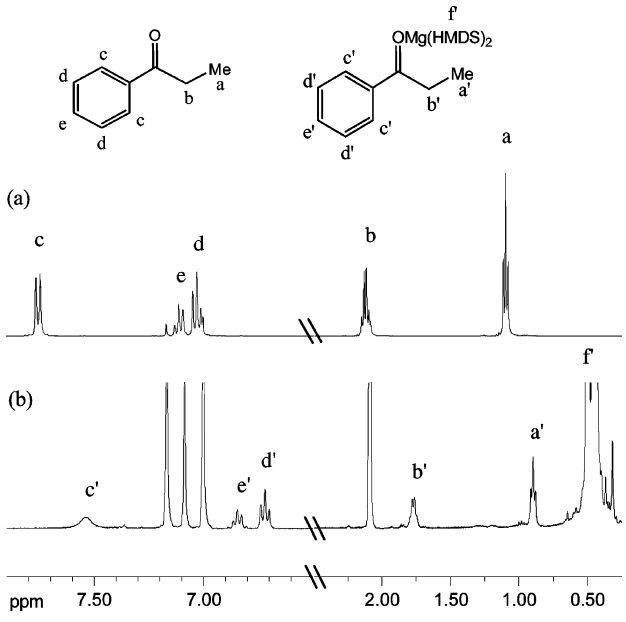

Figure 5. ^{1}H NMR spectra in toluene-d_8 at −86 °C of (a) free propiophenone and (b) the 1:1 pre-enolization complex **2** formed in the presence of excess of Mg(HMDS)$_2$ (0.03 M).

The observation of a carbonyl stretch confirms that enolization has not yet taken place in **2**, and the decrease in energy of the stretch is consistent with complexation of the ketone to magnesium.[49,50]

The composition of intermediate **2** was further investigated by low-temperature NMR. NMR samples were prepared by the addition of approximately 0.25 equiv of propiophenone to 0.03 M solutions of Mg(HMDS)$_2$ in toluene-d_8 at ambient temperature, followed by immediate cooling of the tube in a dry ice/acetone bath. The samples were then inserted into the spectrometer, which was pre-cooled to −86 °C. The ^{1}H NMR spectrum (Figure 5b) indicates quantitative formation of a complex between the ketone and Mg(HMDS)$_2$. A single set of ketone resonances is present, with all of the signals showing an upfield shift compared with the free ketone. The methylene and methyl signals of the ketone move significantly upon complexation, shifting from δ 2.13 to 1.77 ppm, and from 1.10 to 0.90 ppm, respectively. In addition, a new Me$_3$Si singlet appears at δ 0.50 ppm. Integration of the relevant signals reveals a 1:1 stoichiometry of ketone and Mg(HMDS)$_2$ present in complex **2**. The upfield shift in the proton signals was somewhat unexpected considering that the ketone is acting as a Lewis base. However, running the same NMR experiment in dichloromethane-d_2 in place of toluene-d_8 leads to all the ketone signals shifting downfield upon complexation, as expected (Figure S3). It therefore appears that the magnetic anisotropy of the aromatic solvent strongly influences the observed chemical shifts in **2**.

To address the aggregation state of **2**, its molecular size was investigated using diffusion-ordered NMR spectroscopy (DOSY).[51] This technique has found increasing use in determining aggregation states of organometallic species; for example, Williard has recently demonstrated the use of DOSY in differentiating between dimeric and tetrameric forms of ^{n}BuLi in THF.[52] In this case, we used dimeric {Mg(HMDS)$_2$}$_2$ as an internal standard, allowing comparison of complex **2** to a known species under identical conditions. This standardization is essential because the outcomes from triplicate measurements on two separate NMR samples (Table S4) show that, while the *absolute* diffusion coefficients are not reproducible (presumably because of their strong sensitivity to conditions such as temperature gradients),[51] the *relative* diffusion constants of dimeric {Mg(HMDS)$_2$}$_2$ and **2** are reproducible, with the ratio of hydrodynamic volumes of {Mg(HMDS)$_2$}$_2$:**2** of 1.25 ± 0.05. Thus, qualitatively, **2** appears to be significantly smaller than {Mg(HMDS)$_2$}$_2$, in effect limiting its nuclearity to that of a monomer. For more quantitative comparison, the relative volumes of {Mg(HMDS)$_2$}$_2$ (**I**) and the monomeric complex (HMDS)$_2$Mg{η^1-O═C(Ph)CH$_2$CH$_3$} (**II**) were estimated from the optimized geometries of these compounds obtained by density functional theory (DFT) calculations (see below). Using this method, a theoretical $V_{\mathbf{I}}/V_{\mathbf{II}}$ value of 1.43 was obtained, which is in reasonable agreement with the experimentally derived value of 1.25. Given the stoichiometry established by NMR, the presence of coordinated ketone established by IR, and mononuclearity indicated by DOSY, **2** is concluded to be a monomer with a three-coordinate metal center, namely, (HMDS)$_2$Mg{η^1-O═C(Ph)CH$_2$CH$_3$}.

Computational Studies. A computational study was used to further investigate the identity of the reaction intermediate **2** and to probe the energetics of the system.[53] Geometry optimizations and frequency analyses were successfully carried out on the full molecules {Mg(HMDS)$_2$}$_2$ (**I**),[54] (HMDS)$_2$Mg{η^1-O═C(Ph)CH$_2$CH$_3$} (**II**), (HMDS)$_2$Mg{η^1-O═C(Ph)CH$_2$CH$_3$}$_2$ (**III**), and O═C(Ph)CH$_2$CH$_3$ (**IV**) at the HF/6-31G* level of theory.[55] In addition, calculations were attempted on two types of dimers containing a pair of metal-bound propiophenones, one where the ketones bridge the metals, [(HMDS)$_2$Mg{μ-O═C(Ph)CH$_2$CH$_3$}]$_2$,[56] and a second with the ketones acting as terminal Lewis base donors, [(HMDS){CH$_3$CH$_2$C(Ph)═O}Mg(μ-HMDS)]$_2$. Neither dimeric complex optimized to a satisfac-

(49) Lochmann, L.; Trekoval, J. *J. Orgonomet. Chem.* **1975**, *99*, 329.
(50) Klumpp, G. W. *Recl. Trav. Chim. Pays-Bas* **1986**, *105*, 1.
(51) Cohen, Y.; Avram, L.; Frish, L. *Angew. Chem., Int. Ed.* **2005**, *44*, 520.
(52) (a) Keresztes, I.; Williard, P. G. *J. Am. Chem. Soc.* **2000**, *122*, 10228. (b) Jacobson, M. A.; Keresztes, I.; Williard, P. G. *J. Am. Chem. Soc.* **2005**, *127*, 4965.
(53) Frisch, M. J.; et al. *Gaussian 03*; Gaussian, Inc.: Wallingford CT, 2004.
(54) The calculations for {Mg(HMDS)$_2$}$_2$ have previously been reported: Wendell, L. T.; Bender, J.; He, X.; Noll, B. C.; Henderson, K. W. *Organometallics*, published online Sep 7, 2006 http://dx.doi.org/10.1021/om060521g.
(55) (a) Dill, J. D.; Pople, J. A. *J. Chem. Phys.* **1975**, *62*, 2921. (b) Hariharan, P. C.; Pople, J. A. *Theor. Chim. Acta* **1973**, *28*, 213. (c) Hehre, W. J.; Ditchfield, R.; Pople, J. A. *J. Chem. Phys.* **1972**, *56*, 2257.
(56) Mayes, J. M.; Greer, J. C.; Mair, F. S. *New J. Chem.* **2001**, *25*, 262.

Scheme 1. DFT (B3LYP/6-311++G**) Computed Geometry Optimized Structures of **I**−**III** and the Energies (kcal/mol) of the Transformations between the Complexes (selected bond lengths (Å) and angles (deg in italics) are also shown)

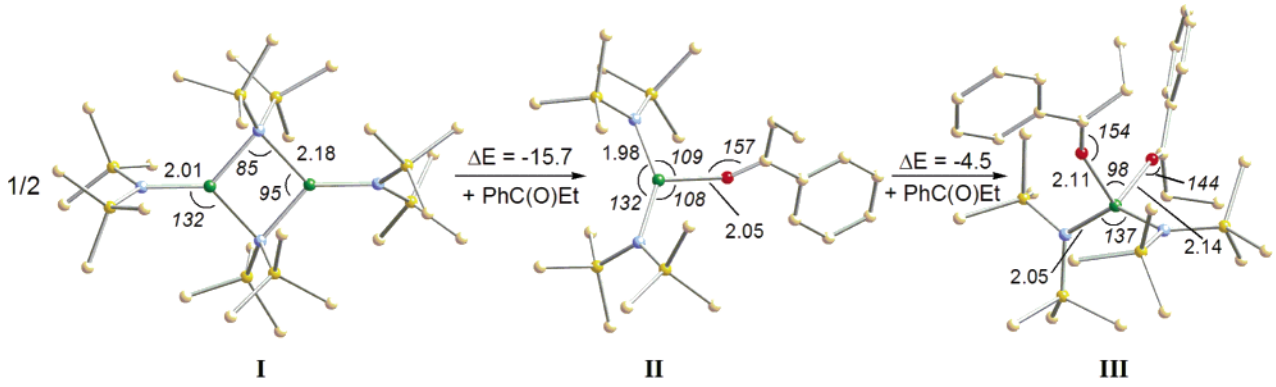

tory geometry minimum but rather resulted in dissociation of the dimer or expulsion of ketone.

To obtain more accurate energies, the Hartree−Fock geometries of **I**−**IV** were used as the starting positions for DFT geometry optimizations run at the B3LYP/6-311++G** level of theory.[57] A summary of these studies is given in Scheme 1. First, the geometries obtained for **I** using both levels of theory compare very well with the crystal structure data for this compound.[54,58] For example, the individual Mg−N distances and the N−Mg−N angles differ by less than 0.05 Å and 1.5°, respectively, between theory and experiment. The absolute energies of the complexes clearly indicate that coordination of propiophenone and deaggregation of dimer **I** to two monomers **II** is highly favorable ($\Delta E = -15.7$ kcal/mol per Mg). Further coordination of ketone to the monomer to give the four-coordinate species **III** is also thermodynamically favorable, but less so ($\Delta E = -4.5$ kcal/mol). Preliminary experimental studies do indicate that **III** can form in the presence of excess ketone, but the calculated energetics clearly indicate that only **II** should be present in the presence of excess $Mg(HMDS)_2$.

Analyses of the bond lengths within the complexes give some insights into their relative stabilities. Going from dimer **I** to monomer **II** leads to shortening of the terminal and bridging Mg−N bonds from 2.01 and 2.18 Å, respectively, to 1.98 Å, along with formation of a relatively short Mg−O bond of 2.05 Å. However, further coordination of propiophenone to **II**, to form **III**, results in slight lengthening of both the Mg−N bonds to 2.05 Å and the Mg−O bonds to 2.10 and 2.15 Å. This is a consequence of increasing the coordination number of the metal from three to four and also increasing the steric encumbrance within the complex. The Mg−O−C angles of 157.5° within **II** and 144.2 and 153.8° within **III** show somewhat bent coordination of the ketone to the metals, although the angles are much more obtuse than would be expected at sp^2-hybridized oxygen. The magnesium centers in **II** and **III** lie close to the plane of the ketone, with Mg−O−C−C(H_2) dihedral angles of 32.3°, and 30.5 and 28.0°, respectively.

Structural Characterization of Model Complexes. In an attempt to prepare model complexes of intermediate **2**, 1 molar equiv of the non-enolizable ketones $^tBu_2CO$ and $^tBuC(O)Ph$ were added to hexane solutions of $Mg(HMDS)_2$. The reactions resulted in the immediate formation of bright yellow solutions that subsequently deposited high quality crystals on cooling. The IR spectra of both complexes indicated the presence of ketone, with C=O stretches at 1661 and 1651 cm^{-1}, respectively. As expected, these signals are shifted to lower frequency compared with those of the free ketones at 1680 and 1676 cm^{-1}, respectively, similar to the decrease of 36 cm^{-1} found between propiophenone-d_2 and **2**-d_2.[49] ^1H NMR spectroscopic studies indicate a 1:1 ratio of metal to ketone present in each case, and single-crystal X-ray diffraction analyses confirm their compositions to be $(HMDS)_2Mg(\eta^1\text{-}O{=}C^tBu_2)$ (**3**, Figure 6) and $(HMDS)_2Mg\{\eta^1\text{-}O{=}C(^tBu)Ph\}$ (**4**, Figure 7).

The complexes adopt monomeric structures with three-coordinate Mg centers. Complexes **3** and **4** are the first examples of magnesium bis(amides) solvated by ketone to be characterized in the solid state.[59] The closest known magnesium analogues to **3** and **4** are the alkoxymagnesium amide $[(HMDS)Mg\{\mu\text{-}OC(H)Ph_2\}(\eta^1\text{-}O{=}CPh_2)]_2$ (**5**)[20] and the magnesium bis(enolate) $Mg_4\{OC(Mes){=}CH_2\}_8\{\eta^1\text{-}O{=}C(Mes)Me\}_2$ (**6**, where Mes = 2,4,6-$Me_3C_6H_2$),[40] both containing terminal ketone bound to four-coordinate magnesium centers. The dimeric ester-solvated lithium amides $[\{\eta^1\text{-}^iPr(^tBuO)CO\}Li(\mu\text{-HMDS})]_2$ (**7**) and $[\{\eta^1\text{-}^tBu(^tBuO)CO\}Li(\mu\text{-HMDS})]_2$ (**8**), which have three-coordinate $M(N)_2O$ coordination spheres similar to those of **3** and **4**, have been reported by Williard.[60] The metrical parameters of **3** and **4** are very similar to each other and are also in reasonable agreement with the calculated geometry of **II** (Table 1). One significant difference between the crystal structures and the

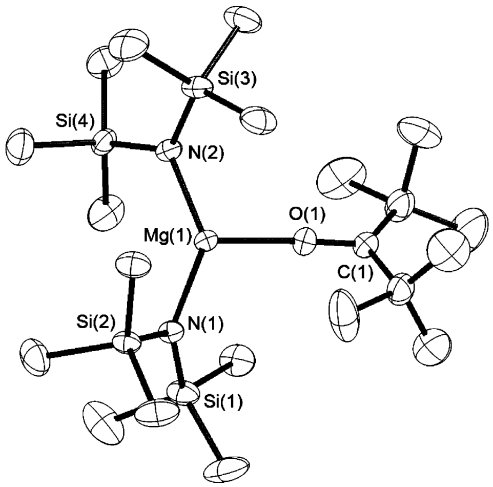

Figure 6. Ellipsoid view of **3** (50% probabilities) with hydrogen atoms removed for clarity.

(57) (a) Becke, D. A. *J. Chem. Phys.* **1993**, *98*, 5648. (b) Miehlich, B.; Savin, A.; Stoll, H.; Preuss, H. *Chem. Phys. Lett.* **1989**, *157*, 200. (c) Lee, C.; Yang, W.; Parr, R. G. *J. Chem. Phys. Rev.* **1988**, *157*, 200.
(58) Westerhausen, M.; Schwarz, W. *Z. Anorg. Allg. Chem.* **1992**, *609*, 39.

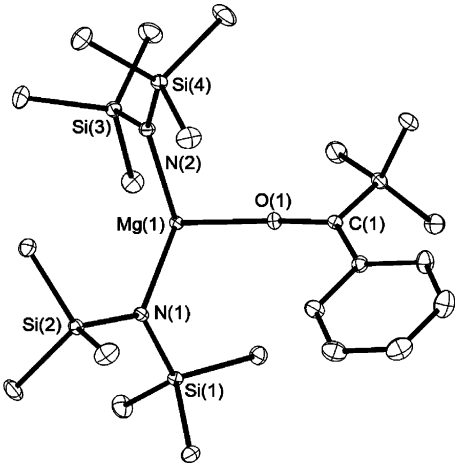

Figure 7. Ellipsoid view of **4** (50% probabilities) with hydrogen atoms removed for clarity.

Table 1. Key Bond Lengths (Å) and Angles (°) in **3** and **4** and Comparisons with the Calculated Values for **II** and **V**

	3	4	II	V
Mg(1)−O(1)	1.970(2)	1.9630(7)	2.054	2.044
Mg(1)−N(1)	1.960(2)	1.9627(8)	1.987	1.987
Mg(1)−N(2)	1.965(2)	1.9665(7)	1.989	1.998
O(1)−C(1)	1.224(3)	1.2321(11)	1.237	1.235
N(1)−Mg(1)−N(2)	136.88(10)	140.99(3)	142.42	141.46
N(1)−Mg(1)−O(1)	112.31(10)	106.14(3)	109.42	109.02
N(2)−Mg(1)−O(1)	110.80(9)	111.83(3)	108.15	109.52
Mg(1)−O(1)−C(1)	177.1(2)	175.16(7)	157.48	172.40
Si(1)−N(1)−Si(2)	123.93(13)	121.65(4)	124.29	124.94
Si(3)−N(2)−Si(4)	124.04(13)	130.89(5)	124.67	122.99

calculations are the Mg(1)−O(1)−C(1) angles, which are almost linear at 175.16(7) and 177.2(2)° in **3** and **4**, whereas a more acute angle of 157.5° is found in **II**. To see whether this reflects an inadequacy of the calculation or a real difference between the less hindered propiophenone and the *tert*-butyl-substituted ketones, a direct comparative calculation was completed for (HMDS)$_2$Mg{η^1-OC(^{t}Bu)Ph} (**V**) at the B3LYP/6-311++G** level of theory. This gave a minimum with metrical parameters very similar to those obtained experimentally for **4**, including a Mg−O−C(1) angle of 172.40° (Table 1). Note that a wide range of M−O−C angles is also observed in the ester-solvated lithium complexes **7** and **8** (144.63−165.15°).[60] These observations indicate that ketone coordination to electropositive metals, such as lithium or magnesium, is highly flexible, with obtuse M−O−C angles common, and with more sterically hindered ketones giving more linear coordination.[61]

The SiN_2 planes of the amides and the R_2CO plane of the ketones form a three-bladed propeller around the central atom, with these planes forming angles of 44.1, 69.0, and 50.5° in **3**, and 50.2, 50.2, and 45.3° in **4**, with respect to the Mg(N)$_2$O coordination plane. This arrangement is typical of metal tris(hexamethyldisilazide) complexes, such as that found in the anions [Mg(HMDS)$_3$]$^-$ and [Ca(HMDS)$_3$]$^-$.[23,62] The complexes thus have helical chirality, though racemization is undoubtedly facile (for example, the methylene protons of the propiophenone in **2** are not diastereotopic, even at −86 °C).

Discussion

Magnesium bis(hexamethyldisilazide), Mg(HMDS)$_2$, reacts with propiophenone in noncoordinating solvents, such as toluene or dichloromethane, over the course of a few minutes at room temperature to form a mixture of (*E*)- and (*Z*)-magnesium enolates. Enolization is therefore substantially slower than with most lithium amides, which typically react within a few seconds at −78 °C.[10d] If the Mg:ketone ratio exceeds 2:1, then the enolate forms dimetallic species (*E*)-**1** and (*Z*)-**1**, which are bridged by one enolate and one amide (eq 2 and Figures 1 and 2). In the presence of more ketone, further deprotonation can take place, leading to amido(enolate) or bis(enolate) formation.[23] Thus, use of excess magnesium appeared likely to simplify the kinetics by isolating the first deprotonation of the ketone by the bis(amide) from reactions involving mixed amido(enolates).

UV−visible spectroscopy reveals that addition of propiophenone to an excess of Mg(HMDS)$_2$ at ambient temperatures leads to an immediate jump in absorbance in the near-UV and concomitant development of a yellow color. That color fades over the course of several minutes, at which point the enolate complex can be observed by NMR. The decay of the near-UV absorbance follows first-order kinetics, and as expected, the observed rate constant is independent of the initial concentration of the deficient reagent, propiophenone. Unexpectedly though, the observed rate constant is also independent of the concentration of the excess reagent, Mg(HMDS)$_2$ (Figure 3). The appearance of optical bands characteristic of neither reactants nor products indicates that a new species, **2**, must be formed by interaction of the ketone with the magnesium amide. The insensitivity of the rate of decay to the concentration of magnesium indicates that the propiophenone is essentially completely converted to **2**. If **2** were in equilibrium with propiophenone, with significant amounts of free ketone still present, then the concentration of **2** would increase with increasing Mg(HMDS)$_2$ concentration, leading to a positive reaction order in [Mg(HMDS)$_2$].

Many lines of evidence indicate that **2** is a monomeric, three-coordinate ketone complex, (HMDS)$_2$Mg{η^1-O=C(Ph)CH$_2$-CH$_3$}: (1) Low-temperature NMR spectra establish that the ketone forms a single complex with a 2:1 ratio of HMDS to ketone, and with the ethyl group still intact, not deprotonated. (2) IR spectra indicate a moderate drop in the carbonyl stretching frequency ($\Delta\nu = -36$ cm^{-1} for the deuterated ketone), consistent with η^1 coordination. (3) Measurement of diffusion constants of **2** using pulsed field-gradient NMR spectroscopy indicates that the molecular size of **2** is most consistent with a monomeric formulation, rather than that of a dimer or higher oligomer. (4) Theoretical calculations are consistent with highly exothermic dissociation of dimeric {Mg(HMDS)$_2$}$_2$ by propiophenone to form three-coordinate monomers, while attempts to find stable minima for ketone-coordinated dimeric species failed. (5) The Mg(HMDS)$_2$ complexes of the non-enolizable

(59) For other examples of monosolvated three-coordinate magnesium bis(amides), see: (a) Tang, Y.; Zakharov, L. N.; Rheingold, A. L.; Kemp, R. A. *Organometallics* **2005**, *24*, 836. (b) Kennedy, A. R.; Mulvey, R. E.; Schulte, J. H. *Acta Crystallogr., Sect. C* **2001**, *57*, 1288. (c) Sebestl, J. L.; Nadasdi, T. T.; Heeg, M. J.; Winter, C. H. *Inorg. Chem.* **1998**, *37*, 1289.

(60) Williard, P. G.; Liu, Q. Y.; Lochmann, L. *J. Am. Chem. Soc.* **1992**, *114*, 348.

(61) A similar observation has been made for the coordination of HMPA to magnesium bis(amides): Clegg, W.; Craig, F. J.; Henderson, K. W.; Kennedy, A. R.; Mulvey, R. E.; O'Neil, P. A.; Reed, D. *Inorg. Chem.* **1997**, *36*, 6238.

(62) (a) Forbes, G. C.; Kennedy, A. R.; Mulvey, R. E.; Rodger, P. J. A. *Chem. Commun.* **2001**, 1400. (b) Honeyman, G. W.; Kennedy, A. R.; Mulvey, R. E.; Sherrington, D. C. *Organometallics* **2004**, *23*, 1197.

Scheme 2. Possible Enolization Mechanisms

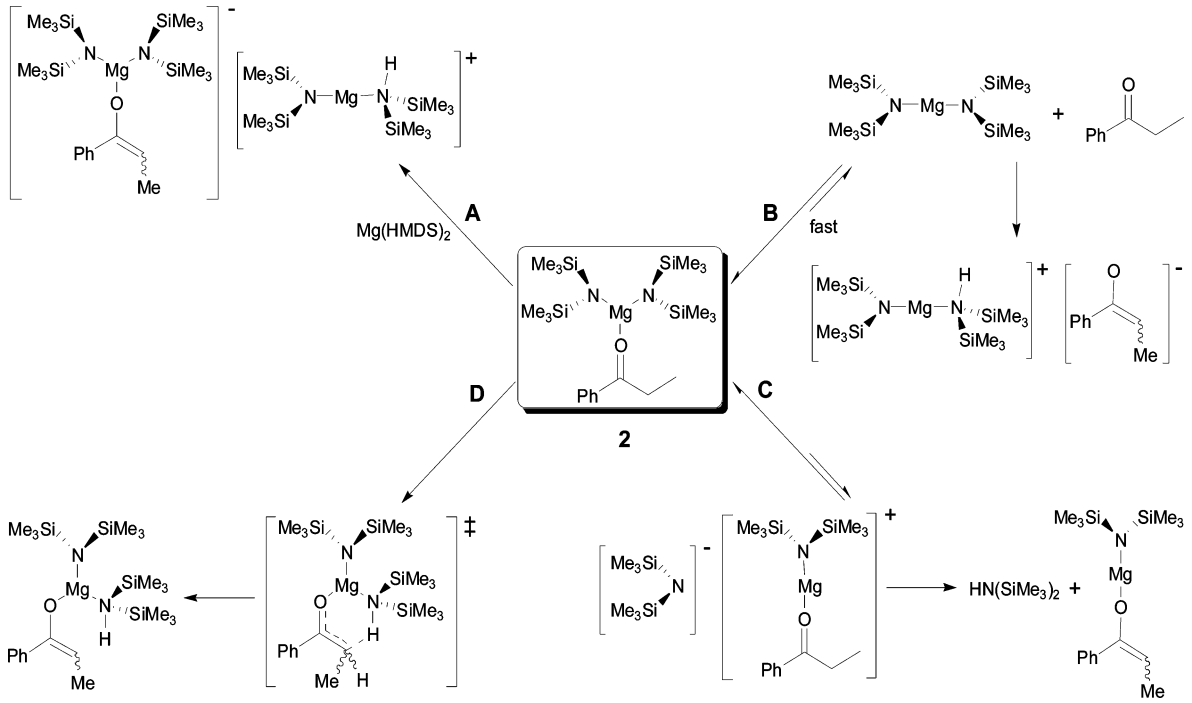

ketones $^{t}Bu_2C{=}O$ and $PhC(O)^{t}Bu$ are shown to be three-coordinate monomers by X-ray crystallography.

Since $(HMDS)_2Mg\{\eta^1\text{-}O{=}C(Ph)CH_2CH_3\}$ (**2**) is the dominant form of propiophenone in the presence of excess $Mg(HMDS)_2$, the decay of the optical transient corresponds to the decay of the complex. The very large rate retardation observed for the $PhCOCD_2CH_3$ complex ($k_H/k_D = 18.9$ at 21 °C) clearly indicates that the rate-determining step for the decay involves proton transfer. Four conceivable mechanisms for the enolization step are shown in Scheme 2. Deprotonation of complexed ketone by exogenous magnesium amide (Mechanism A), whether monomeric or dimeric, is ruled out by the observed insensitivity of the rate to the concentration of free $Mg(HMDS)_2$. Pre-equilibrium dissociation of ketone from the complex, followed by deprotonation of the free ketone by *monomeric* $Mg(HMDS)_2$ (Mechanism B), in contrast, is consistent with the observed rate law since the first-order dependence of the deprotonation step on $[Mg(HMDS)_2]$ would be canceled by the inverse dependence of the concentration of free ketone on $[Mg(HMDS)_2]$. (Deprotonation by dimeric $\{Mg(HMDS)_2\}_2$ would not exhibit such a cancellation and so is ruled out by the observed rate law.) However, if free ketone is deprotonated by free magnesium amide, the transfer of H^+ would result in net charge separation to form an enolate ion pair. The substantial solvent dependence expected for such a reaction is not observed, however, with reactions in toluene ($\epsilon = 2.4$) and dichloromethane ($\epsilon = 8.9$) proceeding at identical rates. Analogous arguments mitigate against dissociation of an amido group and deprotonation of bound ketone within the ion pair (Mechanism C). In contrast, intramolecular proton transfer from coordinated ketone to coordinated amide (Mechanism D) would be expected to show little change in polarity in the transition state. Such an intramolecular reaction is also consistent with the measured moderate negative entropy of activation ($\Delta S^{\ddagger} = -11$ cal/mol·K) of the enolization.

The experimental data thus strongly suggest that enolization takes place intramolecularly within a three-coordinate monometallic intermediate. The net process (Scheme 3) would thus involve initial deaggregation of dimeric $\{Mg(HMDS)_2\}_2$ to form the monomeric, monoketone complex **2**. Complex **2** then undergoes intramolecular proton transfer via a six-membered ring transition state to produce, initially, a three-coordinate amidomagnesium enolate containing a coordinated hexamethyldisilazane. Dissociation of $HN(SiMe_3)_2$ and aggregation of the amido(enolate) with $Mg(HMDS)_2$ leads to the observed products (*E*)-**1** and (*Z*)-**1**.

The intramolecular proton transfer reaction in the rate-determining step is reminiscent of the classic Ireland model of lithium amide-mediated enolization reactions.[63] While Ireland proposed a chair-like structure for the transition state, computational studies support a much less puckered structure.[6f,13a] The observation of a very large primary isotope effect strongly supports such a modified Ireland mechanism. Achieving such a large isotope effect is generally accepted to require a nearly linear C−H−N trajectory, as well as a central transition state (since early or late transition states lead to reduced isotope effects). In fact, large isotope effects, and significant tunneling such as is observed here, are frequently observed for deprotonations of carbon acids with nitrogen bases, with enhanced isotope effects often observed on increasing the steric bulk of the base.[64] The steric enhancement of tunneling is generally ascribed to the bulkier bases requiring a long distance between carbon and nitrogen in the transition state.[65]

The proposed transition structure bears on two important issues of selectivity. First, a cyclic transition state offers an

(63) Ireland, R. E.; Mueller, R. H.; Willard, A. K. *J. Am. Chem. Soc.* **1976**, *98*, 2868.
(64) (a) Lewis, E. S.; Funderburk, L. H. *J. Am. Chem. Soc.* **1967**, *89*, 2322. (b) Caldin, E. F.; Mateo, S. *J. Chem. Soc., Faraday Trans. 1* **1975**, *71*, 1876. (c) Caldin, E. F.; Mateo, S. *J. Chem. Soc., Faraday Trans. 1* **1976**, *72*, 112. (d) Pruszynski, P.; Jarczewski, A. *J. Chem. Soc., Perkin Trans. 2* **1986**, 1117. (e) Pruszynski, P. *Can. J. Chem.* **1987**, *65*, 2160−2163. (f) Leffek, K. T.; Pruszynski, P. *Can. J. Chem.* **1988**, *66*, 1454.
(65) (a) Wolfe, S.; Hoz, S.; Kim, C.-K.; Yang, K. *J. Am. Chem. Soc.* **1990**, *112*, 4186. (b) Kim, Y.; Kreevoy, M. M. *J. Am. Chem. Soc.* **1992**, *114*, 7116.

Scheme 3. Proposed Mechanism of the Enolization of Propiophenone by Mg(HMDS)$_2$

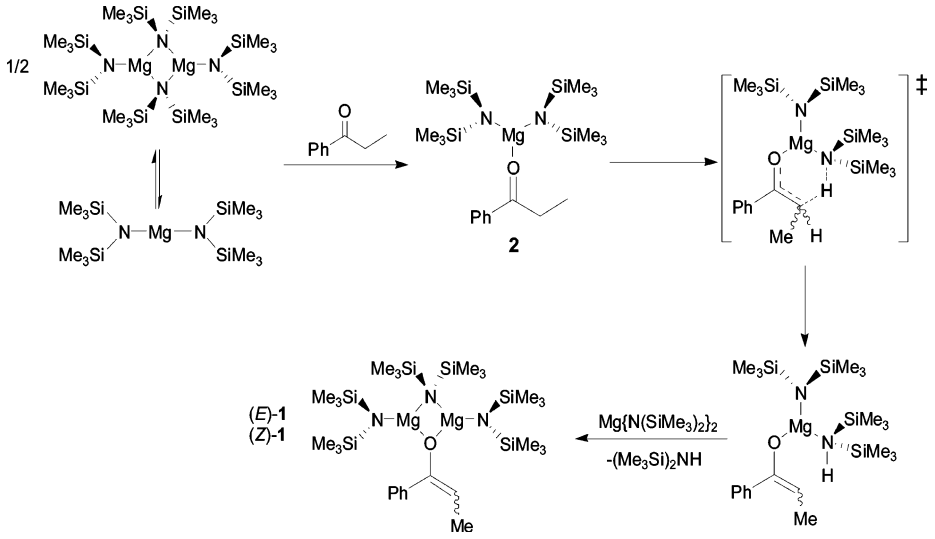

Scheme 4. Cyclic Transition State Structures Leading to (*E*)- and (*Z*)-Enolates

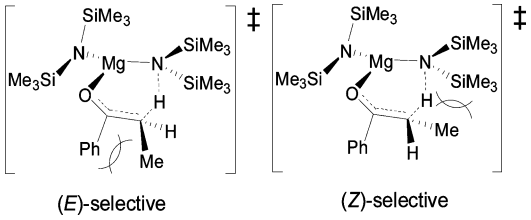

Scheme 5. Possible Conformations of 4-Substituted Cyclohexanones Coordinated to a Magnesium Bis(amide)

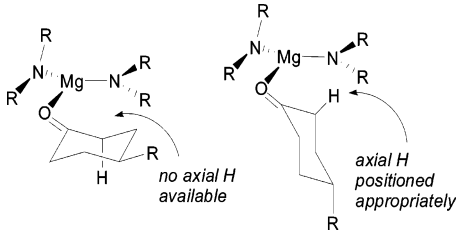

appealing explanation for the relatively high (*E*)-selectivity of enolization of propiophenone by Mg(HMDS)$_2$. Typically, enolizations of propiophenone give predominantly (*Z*)-enolates because of developing $A_{1,3}$ strain between the methyl group and the phenyl group during formation of the (*E*)-enolate.[14,44,63] However, in a cyclic transition state, the methyl group would interact with the trimethylsilyl groups on the amide in the transition state leading to the (*Z*)-enolate, disfavoring it relative to the (*E*)-transition state, where the methyl group is nearly *anti* to the amide (Scheme 4).[24b]

Second, this transition state model also offers an intriguing mechanism for stereoselection in the enantioselective enolization of substituted cyclohexanones by chiral bis(amido)magnesium reagents.[29] The Mg{N(SiMe$_3$)$_2$}$_2$ fragment is intrinsically chiral in the reactive three-coordinate complex since the planes of the amides are canted around the coordination plane like two blades of a three-bladed propeller. Furthermore, the tilt of the amide orients the nitrogen lone pair correctly for proton transfer, as judged from the calculated structures for intramolecular lithium-mediated enolizations.[6f,13a] The helical sense of chirality of the Mg(amide)$_2$ fragment determines which enantiotopic axial proton can be deprotonated; the mismatched proton cannot align with the lone pair on nitrogen (Scheme 5). Thus, any bias provided by the chiral amides that favors one helical conformation over the other could play a determining role in the observed selectivity. This explanation differs significantly over the usual rationalizations in that it emphasizes the interactions *within* the reagent rather than direct interactions between the amide groups of the reagent and the substrate.[66]

(66) Majewski, M.; Wang, F. *Tetrahedron* **2002**, *58*, 4567.

Conclusions

Data from reaction kinetics, spectroscopic characterization of intermediates, and computational and crystallographic structure analyses paint a detailed picture of the mechanism of enolization of propiophenone by the prototypical magnesium bis(amide), magnesium bis(hexamethyldisilazide). The reaction proceeds via initial quantitative formation of the three-coordinate ketone complex (HMDS)$_2$Mg{η^1-O=C(Ph)CH$_2$CH$_3$} (**2**). This complex undergoes rate-limiting intramolecular proton transfer from the ketone to a coordinated amide in a reaction in which tunneling plays a significant role (k_H/k_D = 18.9 at 21.8 °C). An intrinsically chiral, envelope-shaped transition state is proposed, which has important implications for the stereo- and enantioselectivity of magnesium amide-mediated enolization reactions.

Experimental Section

General. All operations were carried out using Schlenk techniques or inside an argon-filled glovebox.[67] All glassware was flame-dried under vacuum before use. Toluene and hexane were dried by passage through copper-based catalyst and molecular sieve columns (Innovative Technology). The ketones were purchased from commercial sources and were distilled over CaH_2 under N_2 prior to use.[68] Me_3SiCl was distilled under a N_2 atmosphere before use. Mg(HMDS)$_2$ was prepared as described previously.[20] Butyllithium was purchased from Aldrich as a 1.6 M solution in hexanes and was standardized by titration against salicylaldehyde phenylhydrazone.[69] Deuterated solvents were purchased from Cambridge Isotope Laboratories and were dried by storage over 4 Å molecular sieves. NMR data were recorded on a Bruker Avance

(67) Shriver, D. F.; Drezdzon, M. A. *Manipulation of Air Sensitive Compounds*; John Wiley and Sons: New York, 1986.
(68) Amarego, W. L. F.; Perrin, D. D. *The Purification of Laboratory Chemicals*, 4th ed.; Butterworth Heinemann: Bath, UK, 2002.
(69) Love, B. E.; Jones, E. G. *J. Org. Chem.* **1999**, *64*, 3755.

DPX-400 instrument at 298 K unless stated otherwise. ^{1}H and ^{13}C spectra were referenced to the residual solvent signals. GC experiments were performed on a Shimadzu GC-17A gas chromatograph fitted with a Rtx-5 fused Crossbond 5% diphenyl/95% dimethyl polysiloxane column (30 m, 0.25 mm i.d., 0.25 umdf), using N_2 as carrier gas. Detection was by flame ionization, and the chromatograms were interpreted using GCsolution software. Elemental analyses were performed by Midwest Microlab, Indianapolis, Indiana.

Spectroscopic Characterization of (*E*)- and (*Z*)-[(HMDS)$_2$Mg$_2$-(μ-HMDS){μ-OC(Ph)=CHCH$_3$}], (*E*)-1 and (*Z*)-1. A ^{1}H NMR sample was prepared at ambient temperature by adding 1 μL of a 2.0 M toluene-d_8 solution of propiophenone (2.03×10^{-6} mol) into an NMR tube charged with 7 mg (2.03×10^{-5} mol) of Mg(HMDS)$_2$ and 0.7 mL of toluene-d_8. The spectrum was taken within a few minutes of mixing the reactants together. Equivalent results are obtained using a stoichiometric ratio of ketone to magnesium (1:2). Previously reported nOe studies were used to assign the stereochemistry of the enolate product;[23] the (*E*)- and (*Z*)-enolates are formed in a 74:26 ratio. **(*E*)-1:** ^{1}H NMR (toluene-d_8) δ 0.23 (s, 36 H, terminal (CH_3)$_3$Si), 0.33 (s, 18H, bridging (CH_3)$_3$Si), 1.62 (d, 3H, J = 7.1 Hz, CHCH_3), 5.33 (q, 1H, J = 7.0 Hz, CHCH$_3$), 7.08 (t, 1H, J = 7.6 Hz, *p*-H), 7.21 (t, 2H, J =7.6 Hz, *m*-H), 7.43 (d, 2H, J =7.6 Hz, *o*-H); ^{13}C NMR spectra were run in methylene chloride-d_2 due to multiple overlapping signals in toluene-d_8; ^{13}C NMR (methylene chloride-d_2) δ 5.95 (terminal (*C*H$_3$)$_3$Si), 6.46 (bridging (*C*H$_3$)$_3$Si), 13.35 (CH*C*H$_3$), 103.84 (*C*HCH$_3$), 125.84 (*o*-C), 128.81 (*p*-C), 129.34 (*m*-C), 139.30 (*i*-C), 151.39 (O*C*=CHCH$_3$). **(*Z*)-1:** ^{1}H NMR (toluene-d_8) δ 0.18 (s, 36 H, terminal (CH_3)$_3$Si), 0.40 (s, 18H, bridging (CH_3)$_3$Si), 1.84 (d, 3H, J = 6.9 Hz, CHCH_3), 5.09 (q, 1H, J = 6.8 Hz, CHCH$_3$), 7.04 (t, 1H, J = 7.6 Hz, *p*-H), 7.17 (t, 2H, J = 7.6 Hz, *m*-H), 7.44 (d, 2H, J = 7.6 Hz, *o*-H); ^{13}C NMR (methylene chloride-d_2) δ 5.82 (terminal (*C*H$_3$)$_3$Si), 6.60 (bridging (*C*H$_3$)$_3$Si), 13.57 (CH*C*H$_3$), 101.59 (*C*HCH$_3$), 128.51 (*o*-C), 128.68 (*p*-C), 129.39 (*m*-C), 140.76 (*i*-C), 152.40 (O*C*=CHCH$_3$).

Crystallization of (*E*)-1 and (*Z*)-1. A Schlenk tube was charged with 0.73 g (2.1 mmol) of Mg(HMDS)$_2$ and 3 mL of toluene. Dropwise addition of 0.13 mL (1 mmol) of propiophenone at ambient temperature resulted in the formation of a bright yellow solution. The solution was allowed to stir for 30 min, during which time the color faded to become colorless. The solvent was removed in vacuo, replaced by 1 mL of hexane, and the mixture filtered through a glass frit. The filtrate was stored at −20 °C, and a crop of colorless crystals was deposited over 3 days. Yield: 0.07 g, 11%. Identical NMR spectra were obtained from the crystals compared with the in situ preparation described above with the exception that the *E*/*Z* ratio was determined to be 20:80. Anal. Calcd for $C_{27}H_{63}Mg_2N_3OSi_6$: C, 48.99; H, 9.60; N, 6.35%. Found: C, 48.98; H, 9.23; N, 6.08%.

Low-Temperature NMR Spectroscopic Analyses of (HMDS)$_2$Mg-{η^1-O=C(Ph)CH$_2$CH$_3$} (2). Samples for the low-temperature studies were prepared as follows: an NMR tube with a screw cap fitted with a Teflon-lined rubber septum was charged with 4.2 mg of Mg(HMDS)$_2$ and 0.6 mL of toluene-d_8 inside a glovebox. The tube was removed from the glovebox and 20 μL of a 0.25 M solution of propiophenone in toluene-d_8 was added via a syringe at ambient temperature. The reactants were mixed thoroughly, and the tube was immediately cooled in a dry ice/acetone bath. The sample was then placed in a −86 °C pre-cooled NMR instrument and its spectrum recorded. ^{1}H NMR (toluene-d_8, 187 K): δ δ 0.50 (s, 36H, SiMe$_3$), 0.90 (t, 3H, J = 6.6 Hz, CH_3), 1.77 (q, 2H, J = 6.7 Hz, CH_2), 6.72 (t, 2H, J = 7.8 Hz, *m*-H), 6.85 (t, 1H, J = 7.8 Hz, *p*-H), 7.54 (br, 2H, *o*-H). A similar procedure was repeated using dichloromethane-d_2 in place of toluene-d_8. ^{1}H NMR (CD$_2$Cl$_2$, 187 K): δ −0.11 (s, 36H, SiMe$_3$), 1.28 (t, 3H, J = 6.8 Hz, CH_3), 3.41 (q, 2H, J = 6.7 Hz, CH_2), 7.59 (t, 2H, J = 7.5 Hz, *m*-H), 7.79 (t, 1H, J = 7.5 Hz, *p*-H), 8.19 (d, 2H, J = 8.2 Hz, *o*-H).

Diffusion NMR Analyses of 2. Samples of **2** were prepared as described above. The NMR spectra were collected on a Bruker Avance DPX-400 instrument equipped with a *z*-axis gradient amplifier. This instrument was operated at 400.13 MHz for ^{1}H observations using a Nalorac 5 mm inverse detection ^{1}H/^{19}F probe with a *z*-axis gradient coil. The LEDBPGS2S pulse sequence was performed with a spectral width of 4006 Hz, and 8 transients were collected for each gradient value. Sinusoidal gradients were used with a total duration of 2.4 ms. The pulsed field-gradients were incremented in 16 steps from 5 up to 90%. Diffusion time was 0.4 s. The eddy current delay was 5 ms. Data processing was accomplished using XWINNMR 2.6.

Measured diffusion coefficients (D) of dimeric {Mg(HMDS)$_2$}$_2$ and **2** were converted to idealized spherical volumes for the Mg(HMDS)$_2$ dimer, V_{std}, and complex **2**, V_2, using the respective hydrodynamic radii (r_s) obtained from the Stokes−Einstein equation.[51,70] The viscosity of toluene at −85.4 °C was estimated using a formula from the literature,[71] and the viscosity of the solution was assumed to be the same as that of the neat solvent. The temperature of the NMR probe was calibrated using 100% methanol.[72]

Quenching Studies. A Schlenk tube under N_2 was filled with 0.17 g (0.5 mmol) of Mg(HMDS)$_2$ and 2.5 mL of toluene. Propiophenone (6.7 μL, 0.05 mmol) was added to the solution and the mixture stirred for 15 min at ambient temperature. Me$_3$SiCl (0.25 mL, 2 mmol) was added, and the solution was cooled to −78 °C. BuLi (1 mL of a 1.6 M solution in hexanes, 1.6 mmol) was added over 1 min followed by 1 mL of THF. The mixture was allowed to warm to room temperature, and a 0.5 mL aliquot of the resulting solution was quenched with 5 mL of saturated aqueous NaHCO$_3$. The quenched reaction mixture was extracted with 5 mL of ether, diluted by THF, and analyzed by GC. The conversion of the ketone to the silyl enol ethers was determined to be >99% with an *E*/*Z* ratio of 72:28. The stereochemical assignments for the silyl enol ethers were made by comparison with authentic samples.[44a]

Synthesis of PhC(O)CD$_2$CH$_3$. A 100 mL round-bottom flask was flushed with argon and charged with 7.90 g (0.059 mol) of propiophenone, a stirring bar, and 30 mL of CH$_3$OD. Sodium methoxide (200 mg, 3.7 mmol) was added via a solids addition tube, and the flask was sealed with a rubber septum. The mixture was stirred for 6 days at ambient temperature, subsequently quenched with cold water (75 mL), and the organics were extracted with Et$_2$O (3 × 40 mL). The organic layer was dried with MgSO$_4$, filtered, and the solvent removed using a rotary evaporator. The ketone was purified by distillation from CaH$_2$ under reduced pressure at 40−42 °C. This cycle was repeated a second time to improve the isotopic enrichment. Yield: 5.81 g, 73.5%. The isotopic purity of PhC(O)CD$_2$CH$_3$ was determined by the ^{1}H NMR spectrum of the product in CDCl$_3$ at 295 K. This indicated a composition of 94% PhC(O)CD$_2$CH$_3$ with the remaining 6% being principally PhC(O)CH(D)CH$_3$, with only a trace of PhC(O)CH$_2$CH$_3$.

IR Spectroscopic Analyses. Spectra were recorded on a Perkin-Elmer Paragon 1000 FTIR spectrometer. Solid samples were prepared as Nujol mulls using KBr plates. Solution samples were prepared in a semi-demountable cell using the deuterated ketone since the half-life of its reaction with Mg(HMDS)$_2$ is relatively long (approximately 43 min). Samples were prepared by mixing 8 μL of PhC(O)CD$_2$CH$_3$ with 0.5 mL of a 0.145 mol/L solution of Mg(HMDS)$_2$ in a sealed vial under argon. The reaction mixture was quickly introduced into the IR cell through a septum and its spectrum recorded. The sample was re-run several times over a 1 h period, and the carbonyl stretch at 1657 cm^{-1} was seen to diminish as expected due to conversion to the enolate.

UV−Vis Spectroscopic Analyses. Spectra were recorded on a Beckman DU 7500 spectrophotometer in a cell block whose temperature was controlled by circulating a water/ethylene glycol mixture through it. The temperature was measured using a digital thermometer which

(70) (a) Crank, J. *The Mathematics of Diffusion*, 2nd ed.; Clarendon: Oxford, 1975. (b) Cussler, E. L. *Diffusion: Mass Transfer in Fluid Systems*; Cambridge University: Cambridge, 1984.
(71) Barlow, A. J.; Lamb, J.; Matheson, A. J. *Proc. R. Soc. London, Ser. A* **1966**, *A292*, 322.
(72) Braun, S.; Kalinowski, H. O.; Berger, S. *100 and More Basic NMR Experiments, A Practical Course*; VCH: New York 1996.

Table 2. Crystallographic Data for Compounds **1**, **3**, and **4**

	1	**3**	**4**
empirical formula	$C_{27}H_{63}Mg_2N_3OSi_6$	$C_{21}H_{54}MgN_2OSi_4$	$C_{23}H_{50}MgN_2OSi_4$
formula weight	662.96	487.33	507.32
temperature, K	100(2)	100(2)	100(2)
wavelength, Å	0.71073	0.71073	0.71073
crystal system	triclinic	monoclinic	monoclinic
space group	$P\bar{1}$	$C2/c$	$P2_1/n$
a, Å	9.0548(5)	21.135(3)	a = 8.3655(2)
b, Å	14.5893(7)	8.3722(10)	b = 20.6214(6)
c, Å	15.6973(8)	37.287(5)	c = 18.7658(5)
α, deg	84.429(2)	90	90
β, deg	83.604(2)	93.029(2)	100.694(1)
γ, deg	79.376(2)	90	90
volume, Å^3	2019.20(18)	6588.4(14)	3181.03(15)
Z	2	8	4
density (calcd), g/cm^3	1.090	0.979	1.059
absorption coefficient, mm^{-1}	0.261	0.213	0.223
F(000)	724	2142	1112
crystal size, mm	0.48 × 0.37 × 0.32	0.49 × 0.45 × 0.28	0.46 × 0.43 × 0.16
ϕ range, °	1.31 to 27.88	1.93 to 28.88	1.48 to 31.56
index ranges	$-11 \le h \le 11$, $-19 \le k \le 19$, $-20 \le l \le 20$	$-28 \le h \le 28$, $-10 \le k \le 11$, $-46 \le l \le 50$	$-12 \le h \le 12$, $-30 \le k \le 30$, $-26 \le l \le 27$
reflections collected	131789	27124	116269
independent reflections	9578 [R(int) = 0.0430]	8604 [R(int) = 0.0254]	10635 [R(int) = 0.0367]
max and min transmission	0.9212 and 0.8856	0.94 and 0.91	0.9652 and 0.9044
data/restraints/parameters	9578/2/385	8604/1/327	10635/0/298
Goodness-of-fit on F^2	1.108	1.325	1.028
R_1 [$I > 2\sigma(I)$]	0.0377	0.0851	0.0286
$wR2$ (all data)	0.1106	0.2021	0.0791
largest diff. peak and hole, e·Å^{-3}	0.612 and −0.444	0.427 and −0.419	0.459 and −0.176

was placed in a solvent-filled cuvette within the sample holder. Samples were contained in quartz cuvettes with screw-caps fitted with PTFE-faced silicone rubber septa.

A typical sample was prepared as follows: inside a glovebox, a 50 mL volumetric flask was charged with 0.8270 g of Mg(HMDS)$_2$ and filled with dry toluene. This was then used as a standard solution for the reactions. Each run used 3.0 mL samples of this solution, which were placed into cuvettes, capped, and the caps covered with Parafilm. The cuvettes were taken out of the glovebox and loaded into the UV−vis sample holder. The temperature of the circulating bath was then adjusted and the sample allowed to thermally equilibrate for approximately 20 min. After this time, 30 μL of a 0.292 M solution of propiophenone was added to the cuvette, and data were collected immediately. Spectra were acquired at 330 nm for at least 5 half-lives.

For the reactions of PhC(O)CH$_2$CH$_3$, absorbance versus time data were fit to the formula $A = A_f + (A_0 - A_f)\exp(-k_{obs}t)$ using the program Origin 6.1 (OriginLab Corporation, Northampton MA). For reactions of PhC(O)CD$_2$CH$_3$, data were fit to $A = 0.06(A_0 - A_f)\exp(-k^{H}_{obs}t) + 0.94(A_0 - A_f)\exp(-k^{D}_{obs}t) + A_f$, where both k^{H}_{obs} and k^{D}_{obs} were allowed to vary. Values of k^{H}_{obs} agreed, within experimental error, with the $0.5 \times k_{obs}$ measured under similar conditions for the protio compound (as expected from a statistical factor of 2).

Synthesis of (HMDS)$_2$Mg(η^1-OC^{t}Bu$_2$) (3). A Schlenk tube under argon was charged with 0.69 mL (4 mmol) of 2,2,4,4-tetramethyl-3-pentanone, and a solution of Mg(HMDS)$_2$ (4 mmol, 1.38 g) in hexane (10 mL) was added by syringe to give a light yellow solution. The solution was cooled to −20 °C, and a crop of colorless crystals precipitated overnight. Yield: 0.37 g, 19%. ^{1}H NMR (toluene-d_8): δ 0.30 (s, 36H, Si(CH_3)$_3$), 0.90 (s, 18H, C(CH_3)$_3$). ^{13}C NMR (toluene-d_8): δ 6.10 (Si(CH_3)$_3$), 27.84 (C(CH_3)$_3$), 47.44 (C(CH$_3$)$_3$), 236.33 (O=C). IR (cm^{-1}): ν 1661 (C=O). Anal. Calcd for $C_{21}H_{54}MgN_2OSi_4$: C, 51.76; H, 11.17; N, 5.75%. Found: C, 50.75; H, 10.83; N, 5.90%.

Synthesis of (HMDS)$_2$Mg{η^1-OC(^{t}Bu)Ph} (4). A Schlenk tube was charged with 0.35 g (1 mmol) of crystalline Mg(HMDS)$_2$ and 1 mL of hexane. 2,2′-Dimethylpropiophenone (0.17 mL, 1 mmol) was added dropwise to produce a light yellow solution. After stirring for 15 min at ambient temperature, the mixture was stored at 0 °C, and colorless crystals formed over a period of 2 days. Yield: 0.20 g, 39%. ^{1}H NMR (toluene-d_8): δ 0.29 (s, 36H, Si(CH_3)$_3$), 1.11 (s, 9H, C(CH_3)$_3$), 7.03−7.05 (m, 3H, *m*- and *p*-H), 7.87 (d, 2H, J = 7.2 Hz, *o*-H). ^{13}C NMR (toluene-d_8): δ 5.91 (Si(CH_3)$_3$), 28.10 (C(CH_3)$_3$), 45.47 (C(CH$_3$)$_3$), 129.09 (*m*-C), 130.27 (*o*-C), 135.07 (*p*-C), 135.46 (*i*-C), 219.86 (C=O). IR (cm^{-1}): ν 1651 (C=O). Anal. Calcd for $C_{23}H_{50}MgN_2OSi_4$: C, 54.51; H, 9.95; N, 5.53%. Found: C, 54.80; H, 9.59; N, 5.26%.

Computational Details. The Gaussian 03 series of programs was used for the geometry optimization calculations for **I**−**V**.[53] No symmetry constraints were imposed, and the molecules were allowed to freely optimize at the HF/6-31G* level using related crystal structure data as starting geometries.[55] The geometries were verified as true minima using frequency analyses. The ab initio derived geometries of **I**−**V** were re-optimized at the B3LYP/6-311++G** level of theory to obtain more accurate absolute energy data.[57] Molecular volumes for **I**−**III** were calculated using the Spartan 04 program.[73]

X-ray Crystallography. Single crystals of **1**, **3**, and **4** were grown according to the experimental procedures outlined above and were examined under Infineum V8512 oil. In each case, the datum crystal was affixed to either a thin glass fiber atop a tapered copper mounting pin or a Mitegen mounting loop and transferred to the 100 K nitrogen stream of a Bruker APEX diffractometer equipped with an Oxford Cryosystems 700 series low-temperature apparatus. Cell parameters were determined using reflections harvested from three sets of 12 0.5° ϕ scans. The orientation matrix derived from this was transferred to COSMO[74] to determine the optimum data collection strategy requiring a minimum of 4-fold redundancy. Final cell parameters were refined using reflections harvested from the data collection with $I \ge 10\sigma(I)$. All data were corrected for Lorentz and polarization effects, and runs were scaled using SADABS.[75]

The structures were solved and refined using SHELXTL.[76] Structure solution was by direct methods. Non-hydrogen atoms not present in

(73) *Spartan 04*; Wavefunction Inc.: Irvine, CA, 2004.
(74) Bruker-Nonius AXS (2005), APEX2, and COSMO; Bruker-Nonius AXS: Madison, Wisconsin.
(75) Sheldrick, G. M. 2004. *SADABS*; Bruker-Nonius AXS: Madison, Wisconsin.
(76) Sheldrick, G. M. *SHELXTL*; University of Göttingen: Göttingen, Germany.

the direct methods' solution were located by successive cycles of full-matrix least squares refinement on F^2. All non-hydrogen atoms were refined with parameters for anisotropic thermal motion. Hydrogen atoms were placed at idealized geometries and allowed to ride on the position of the parent atom. Hydrogen thermal parameters were set to 1.2 times the equivalent isotropic U of the parent atom, 1.5 times for methyl hydrogens. Table 2 lists the key crystallographic parameters.

The crystal structure of **1** exhibits disorder in the enolate functional group. Carbon C(21) presented two sites, the (*E*)- and (*Z*)-isomeric forms. Alternate positions were located and refined for C(20) and C(21) (C(20′) and C(21′)). The site occupancies were refined so that the total of each part equaled 1. The site occupancy factor of the major orientation is 0.779(6). Because of the disorder, thermal factors for C20 and C20′ were set to be equal using EADP from XL.[76] Also, the C19−C20 and C19−C20′ distances were restrained to be similar to the SADI command. Distances C20−C21 and C20′−C21′ were similarly restrained. In compound **3**, the carbon atoms of the *tert*-butyl groups were disordered. Atoms C(7), C(8), and C(9) were modeled as having two-site disorder. The site occupancy of the major component refined to 0.643(12). C(3), C(4), and C(5) were also modeled as having two-site disorder. The site occupancy of the major component refined to 0.525(13). Parameters for thermal motion of the methyl carbons of the ketone were restrained to be equivalent using the EADP function of XL.[76] Compound **4** was well-behaved on refinement.

Acknowledgment. K.W.H. and X.H. gratefully acknowledge the National Science Foundation for support (CHE03-45713). We also thank the National Science Foundation for instrumentation support (CHE04-43233).

Supporting Information Available: Crystallographic data for **1**, **3**, and **4** in CIF format; the complete list of authors for refs 6c and 53; tables summarizing (i) bond lengths and angles for **1**, (ii) the kinetic data, and (iii) the diffusion NMR experiments; Eyring plot of the reaction of $Mg(HMDS)_2$ with propiophenone; plot of absorbance versus time for the disappearance of intermediate **2**; ^{1}H NMR spectra of free propiophenone and intermediate **2** in dichloromethane-d_2; and details of the calculations. This material is available free of charge via the Internet at http://pubs.acs.org.

JA064927W